Volume 8, Issue 6, 2018, 3682 - 3687 **ISSN 2069-5837**

Biointerface Research in Applied Chemistry

www.BiointerfaceResearch.com

Original Research Article **Open Access Journal**

Received: 10.10.2018 / Revised: 29.11.2018 / Accepted: 10.12.2018 / Published on-line: 15.12.2018

Effect of alkaline elements on the structure and electronic properties of glycine

Rania Badry [1], Amina Omar [2], Haitham Mohammed [3], Doha Adel Awies Mohamed [1], HananElhaes [1], Ahmed Refaat [4], Medhat Ibrahim [4, *]

[1]Physics Department, Faculty of Women for Arts, Science and Education, Ain Shams University, 11757 Cairo, Egypt
[2]Physics Department, Biophysics Branch, Faculty of Science, Ain Shams University, 11566, Cairo, Egypt
[3]Fellow of Higher Nasser Military Academy, Instructor, School of EAS, Nile University
[4]Spectroscopy Department, National Research Centre, 33 El-Bohouth Str. 12622 Dokki, Giza, Egypt

*corresponding author e-mail address: ***medahmed6@yahoo.com***

ABSTRACT

This study is introduced to investigate the activity of Glycine as a result of decoration with alkali metals such as Li, Na and K, and with alkaline earth metals like Be, Mg and Ca. Density functional theory (DFT) quantum mechanical calculations are performed to confirm total dipole moment (TDM), HOMO/LUMO band gap energy, electrostatic potentials (ESP) and geometrical parameters (bond length and bond angles) for all models under study. Due to the decoration, TDM increased, HOMO/LUMO band gap energy increased, molecular ESP is changed, bond length increased, and also bond angles changed due to the interaction that occurred between Glycine and metals.

Keywords: *DFT, TDM, HOMO/LUMO band gap energy and geometrical parameters.*

1. INTRODUCTION

Amino acids are the building units of protein structure, containing both a basic amino group and an acidic (COOH) group [1]. Alanine, for example, which is an aliphatic amino acid and considered the simplest α-amino acid, its methyl group never directly interfere in protein function, and is still a topic of interest [2-5]. Furthermore, for such small molecule, experimental together with computational efforts are gathered to study its molecular structure [6]. Glycine (Gly), which is the simplest possible amino acid, contains a single hydrogen atom that is located at its side chain. It was discovered as early as 1820 by Henri Braconnot [7]. It is considered an important amino acid in the central nervous system [8]. Gly is known earlier that it serves as a neurotransmitter at many inhibitory synapses in the spinal cord and brainstem [9-10].

Recently, Gly, which is inexpensive, shows emerging applications as an efficient and eco-friendly lixiviant for copper leaching [11-13]. Carboxyl group is among the most important reactive functional groups in chemistry, biology and the environment [14,15]. This dedicates any structure containing carboxyl group for extensive studies theoretically and experimentally [16]. Computational methods based on quantum mechanics are supporting molecular spectroscopic methods for studying the molecular structure of proteins [17]. For example, the interaction between heavy metals and proteins is elucidated with molecular modeling and experimental molecular spectroscopy [18]. The interaction between metal ions and amino acids is still of concern for many researchers [19-21]. Based on these considerations, molecular modeling is a useful tool for studying many systems and molecules to explain the experimental behavior and/or re-design the experimental approaches [22-25]. Accordingly, this class of calculations is widely applied for all classes of molecular systems to investigate their chemical, thermal and biological properties.

In the present work, B3LYP/6-31g(d,p) was utilized to optimize Gly then Gly interacted with Na, K, Ca, Mg, Fe and Zn respectively. The TDM, HOMO/LUMO band gap energy and vibrational characteristics were calculated at the same level of theory.

2. EXPERIMENTAL SECTION

Calculation Details. Building a model molecule for Gly and Gly interacted with alkali metals such as Li, Na and K, and with alkaline earth metals like Be, Mg and Ca was presented in our study. All calculations were made on a personal computer at Spectroscopy Department, National Research Centre, Egypt using Gaussian 09 program [26]. All model molecules are optimized with DFT quantum mechanical calculations at B3LYP/6-31G (d,p) basis set [27-29]. The TDM; HOMO/LUMO band gap energy; ESP and geometrical parameters (bond length and angles) are introduced for all structures.

3. RESULTS SECTION

Model molecules representing Gly and Gly interacted with alkali metals such as Li, Na and K and with alkaline earth metals like Be, Mg and Ca are presented as shown in figure 1. Gly is supposed to be decorated with Li, Na, K, Be, Mg and Ca. There are three different active sites through which we can describe the mechanism of interaction between Gly and the different groups of

metals. Firstly, Gly can be interacted with the two groups of metals, alkali and alkaline earth metals, through hydroxyl group, middle NH group and finally through the amide group. Figures 1, 2 and 3 show the optimized structures describing Gly and Gly interacted with Li, Na, K, Be, Mg and Ca through hydroxyl group, middle NH group and amide group respectively. All calculations are performed using DFT quantum mechanical method at B3LYP/6-31G (d,p) basis set. The knowledge of TDM and HOMO/LUMO band gap energy helps us to indicate the reactivity of the model, therefore TDM as Debye and HOMO/LUMO band gap energy ΔE as eV are calculated at the same level of theory at B3LYP/6-31G (d,p).

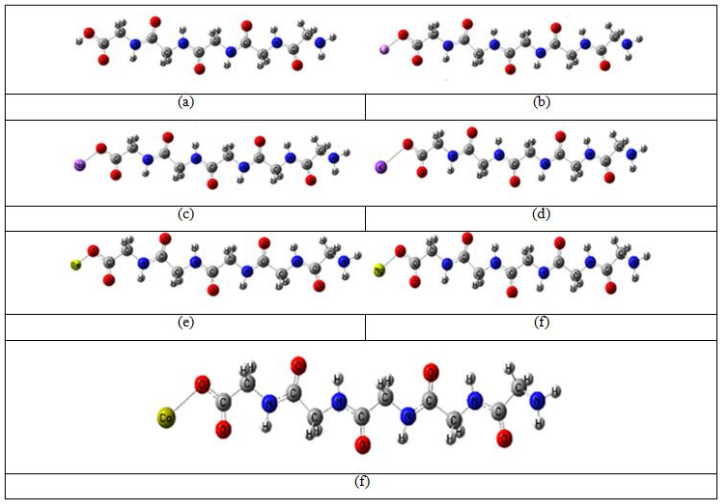

Figure 1. B3LYP/6-31G (d,p) optimized structures of a:Gly, b:Gly-Li, c:Gly-Na, d:Gly-K, e:Gly-Mg and g:Gly-Ca through hydroxyl group.

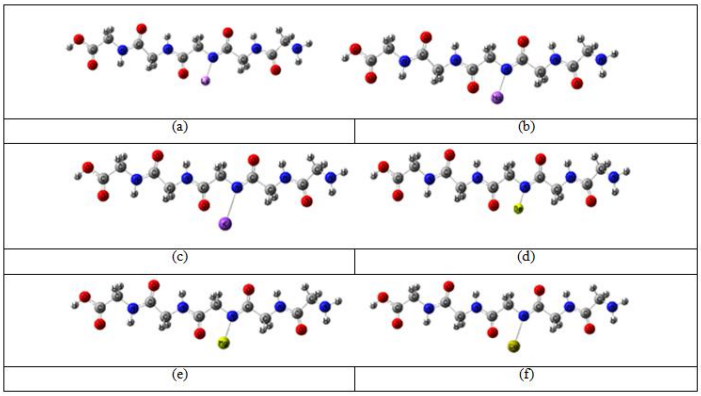

Figure 2. B3LYP/6-31G (d,p) optimized structures of a: Gly-Li, b:Gly-Na, c:Gly-K, d:Gly-Be, e:Gly-Mg and f:Gly-Ca through middle NH group.

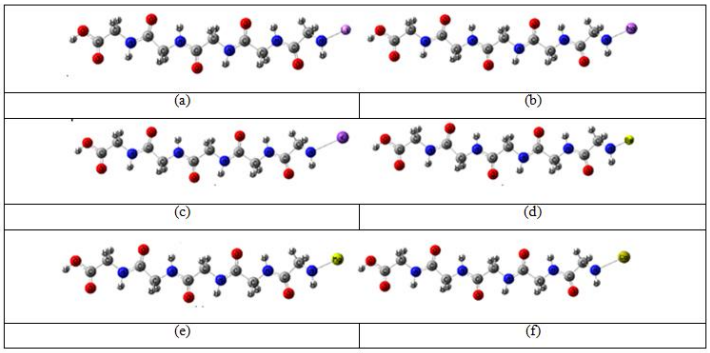

Figure 3. B3LYP/6-31G (d,p) optimized structures of a: Gly-Li, b:Gly-Na, c:Gly-K, d:Gly-Be, e:Gly-Mg and f:Gly-Ca through terminal amide group.

Although HOMO/LUMO band gap energy and TDM are physical quantities, but they reflect the reactivity of the studied structures as stated earlier [30-31].

Table 1 presents TDM and HOMO/LUMO band gap energy for a: Gly, b: Gly-Li, c: Gly-Na, d: Gly-K, e: Gly-Be, f: Gly-Mg and g: Gly-Ca through hydroxyl group.

Table 1. B3LYP/6-31G (d,p) calculated TDM as Debye; HOMO/LUMO band gap energy (ΔE) as eV for the studied structures: a: Gly, b: Gly-Li, c: Gly-Na, d: Gly-K, e: Gly-Be, f: Gly-Mg and g: Gly-Ca through hydroxyl group.

Structure	TDM	ΔE
Gly	9.2026	5.2829
Gly-Li	12.5117	4.5152
Gly-Na	15.0343	3.9269
Gly-K	17.2778	4.1231
Gly-Be	9.2980	3.3721
Gly-Mg	8.8557	2.4422
Gly-Ca	10.6287	1.7693

In the case of terminal connected through the hydroxyl group as shown in figure 4, TDM increased with increasing atomic number of the doping metal of the same group (alkali metals or alkaline earth metals), but HOMO/LUMO band gap energy decreased with increasing atomic number of metals present in the same group. Also from our calculations, we noticed that in the case of alkali metals, the highest value of TDM equals 17.2778 Debye that is for Gly-K and the lowest value of HOMO/LUMO band gap energy equals 3.9269 eV that is for Gly-Na, whereas the highest value of TDM for alkaline earth metals equals 10.6287 Debye and the lowest value of HOMO/LUMO band gap energy equals 1.7693 eV that is for Gly-Ca.

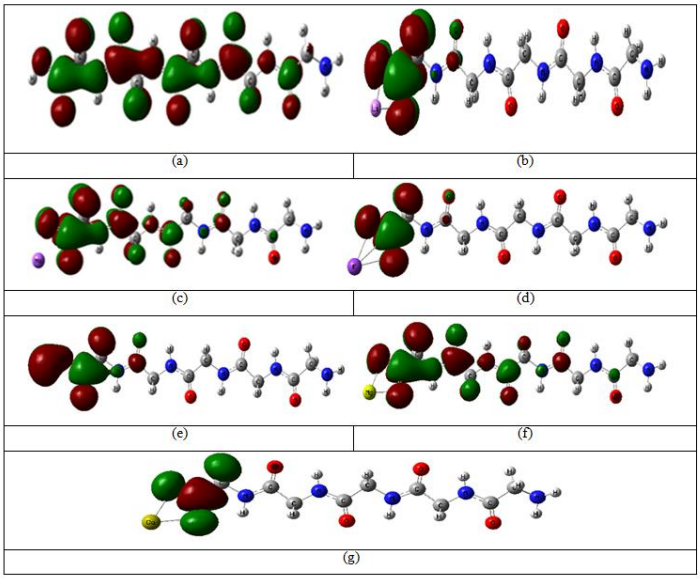

Figure 4. B3LYP/6-31G (d,p) HOMO/LUMO band gap energy of a:Gly, b:Gly-Li, c:Gly-Na, d:Gly-K, e:Gly-Be, f:Gly-Mg and g:Gly-Ca through hydroxyl group.

Figure 5 illustrates the HOMO/LUMO band gap energy of Gly interacted with Li, Na, Be, Mg and Ca. As a result of interaction through the middle NH group, the HOMO/LUMO band gap energy of Gly interacted with metals is higher than that of Gly but TDM is decreased when we go downward the group. On the other hand, HOMO/LUMO band gap energy decreased slightly in the case of alkali metals but decreased significantly in the case of alkaline earth metals as presented in table 2 which illustrates TDM and HOMO/LUMO band gap energy of a: Gly-Li, b: Gly-Na, c:

Gly-K, d: Gly-Be, e: Gly-Mg and f: Gly-Ca through middle NH group.

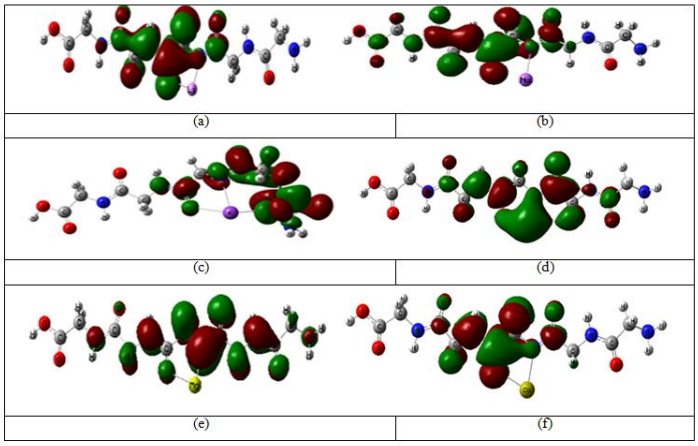

Figure 5. B3LYP/6-31G (d,p) HOMO/LUMO band gap energy of a: Gly-Li, b:Gly-Na, c:Gly-K, d:Gly-Be, e:Gly-Mg and f:Gly-Ca through middle NH group.

Table 2. B3LYP/6-31G (d,p) calculated TDM as Debye; HOMO/LUMO band gap energy (ΔE) as eV for the studied structures: a: Gly-Li, b: Gly-Na, c: Gly-K, d: Gly-Be, e: Gly-Mg and f: Gly-Ca through middle NH group.

Structure	TDM	ΔE
Gly-Li	12.8016	4.6945
Gly-Na	11.5028	3.9035
Gly-K	7.4291	4.1011
Gly-Be	14.5799	2.3614
Gly-Mg	13.2870	2.4537
Gly-Ca	12.3667	1.7641

Table 3 presents TDM and HOMO/LUMO band gap energy values of a: Gly-Li, b: Gly-Na, c: Gly-K, d: Gly-Be, e: Gly-Mg and f: Gly-Ca through the terminal amide group. Results indicated that TDM slightly increased from 9.2026 Debye to 10.7597 Debye, and HOMO/LUMO band gap energy decreased from 5.2829 eV to 1.6871 eV. TDM values followed the sequence 7.4406, 10.7597 and 9.5527 Debye for Gly-Li, Gly-Na and Gly-K respectively, whereas for Gly-Be, Gly-Mg and Gly-Ca, TDM values are 10.5810, 8.5148 and 7.3825 Debye respectively, such that for alkaline earth metals, TDM decreases with increasing atomic number of metals.

Table 3. B3LYP/6-31G (d,p) calculated TDM as Debye; HOMO/LUMO band gap energy (ΔE) as eV for the studied structures: a: Gly-Li, b: Gly-Na, c: Gly-K, d: Gly-Be, e: Gly-Mg and f: Gly-Ca through terminal amide group.

Structure	TDM	ΔE
Gly-Li	7.4406	2.7753
Gly-Na	10.7597	2.5307
Gly-K	9.5527	1.9255
Gly-Be	10.5810	3.6812
Gly-Mg	8.5148	2.3018
Gly-Ca	7.3825	1.6871

Figure 6 presents the HOMO/LUMO band gap energy of a: Gly-Li, b: Gly-Na, c: Gly-K, d: Gly-Be, e: Gly-Mg and f: Gly-Ca through the terminal amide group. The values of HOMO/LUMO band gap energy for alkali metals are in the sequence of 2.7753 eV for Gly-Li, 2.5307 eV for Gly-Na and 1.9255 eV for Gly-K, but for alkaline earth metals, HOMO/LUMO band gap energy values became 3.6812 eV for Gly-Be, 2.3018 eV for Gly-Mg and 1.6871 eV for Gly-Ca.

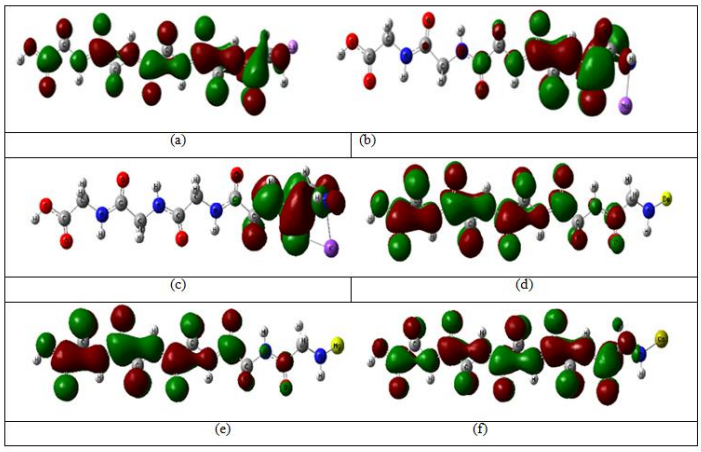

Figure 6. B3LYP/6-31G (d,p) HOMO/LUMO band gap energy of a: Gly-Li, b:Gly-Na, c:Gly-K, d:Gly-Be, e:Gly-Mg and f:Gly-Ca through terminal amide group.

ESP values were also calculated for all studied model molecules as contour and as a total surface area at the same quantum mechanical calculations. Figures 7 and 8 present the ESP as contour and as total surface area for a: Gly, b: Gly-Li, c: Gly-Na, d: Gly-K, e: Gly-Be, f: Gly-Mg and g: Gly-Ca hydroxyl middle. It is clear that the electronegativity of Gly was influenced by the presence of alkali and alkaline earth metals. Also figures 9, 10, 11 and 12 present the ESP as contour and as total surface area in the other two mechanisms of interaction, through middle NH group and through terminal amide group, for a: Gly-Li, b: Gly-Na, c: Gly-K, d: Gly-Be, e: Gly-Mg and f: Gly-Ca.

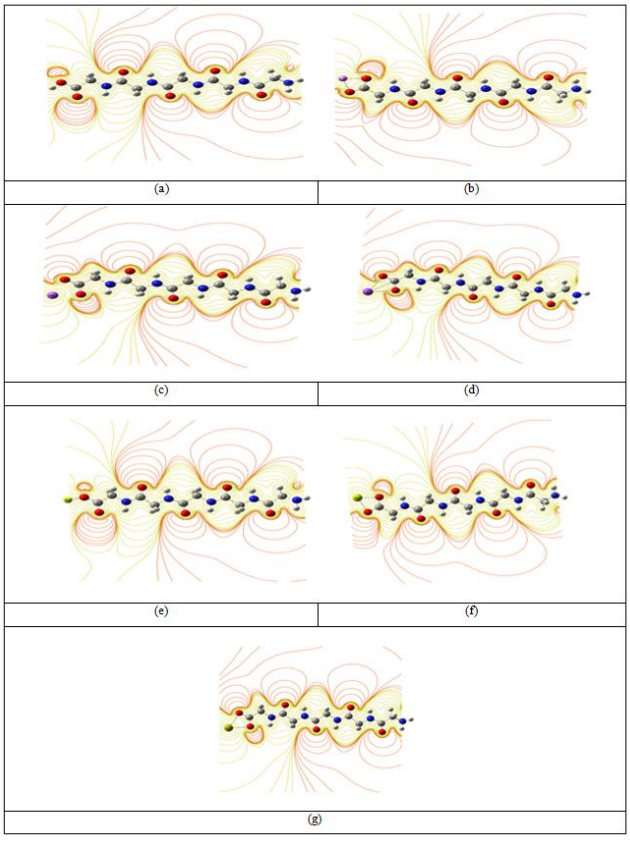

Figure 7. B3LYP/6-31G (d,p) ESP as contour of a: Gly, b: Gly-Li, c: Gly-Na, d: Gly-K, e: Gly-Be, f: Gly-Mg and g: Gly-Ca through hydroxyl group.

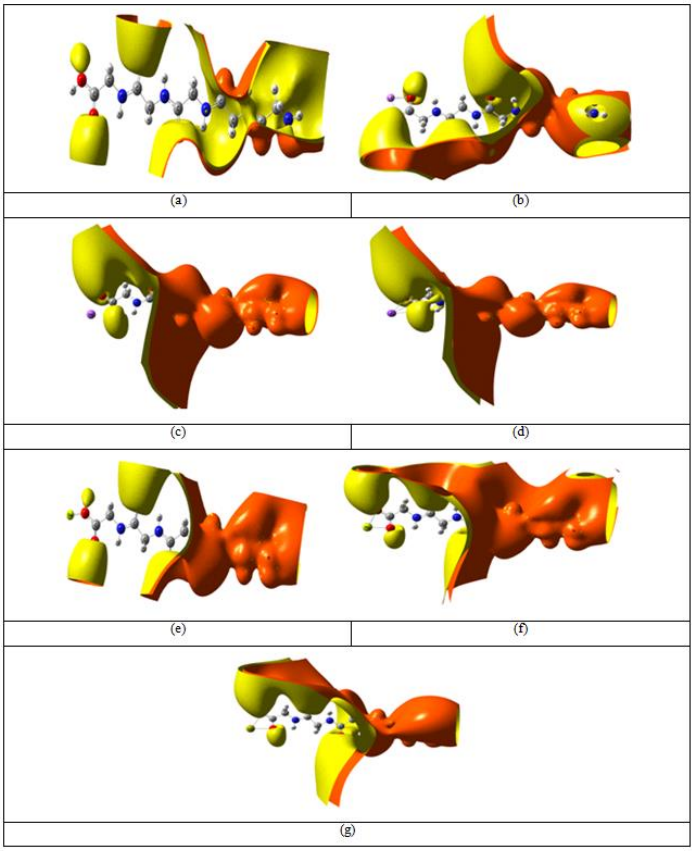

Figure 8. B3LYP B3LYP/6-31G (d,p) ESP as total surface area of a: Gly, b: Gly-Li, c: Gly-Na, d: Gly-K, e: Gly-Be, f: Gly-Mg and g: Gly-Ca through hydroxyl group.

As a result of the interaction between the studied metals and Gly, there is a change in both bond length and bond angle for all model molecules. Table 4 presents the change in bond length and bond angle for all structures in the three mechanisms of interaction, through hydroxyl group, middle NH group and terminal amide group. The bond length in the three different sites of interaction increased from 0.9725 Å to 1.8671, 2.1962 and 2.5378 Å for Li, Na and K respectively, and increased to 1.4470, 2.0674 and 2.3686 Å for Be, Mg and Ca respectively for the interaction through the hydroxyl group. On the other hand, the bond angles changed and decreased from 107.013° to 82.862°, 87.288° and 91.253° for Li, Na and K respectively, and changed to135.910°, 87.952° and 91.166° for Be, Mg and Ca. For the interaction through the middle NH group, the bond length increased from 1.0149 Å to 1.8660, 2.2037 and 2.6840 Å for Li, Na and K respectively, and to 1.1689, 2.0490 and 2.4011 Å for Be, Mg and Ca respectively. There are two bond angles corresponding to this interaction, X38N20C3 and X38N20C19, where X is the interacting metal. The bond angle of X38N20C3 changed from 123.114° to 140.498°, 129.952°, 109.316°, 134.896°, 134.240° and 132.193° for Li, Na, K, Be, Mg and Ca respectively, and the bond angle of X38N20C19 changed from 114.764° to 106.212°, 110.679°, 113.377°, 110.628°, 112.919° and 115.978° for Li, Na, K, Be, Mg and Ca respectively. Finally, for the interaction through the terminal amid group, the bond length changed and increased from 1.0191 Å to 1.7496, 2.1971 and 2.5617 Å for Li, Na and K respectively, and increased to 1.4991, 1.9259 and 2.2550 Å for Be, Mg and Ca respectively, while bond angles are changed and increased from 107.697° to 117.505°, 108.770°, 120.124°, 119.740°, 117.594° and 116.256° for Li, Na, K, Be, Mg and Ca respectively.

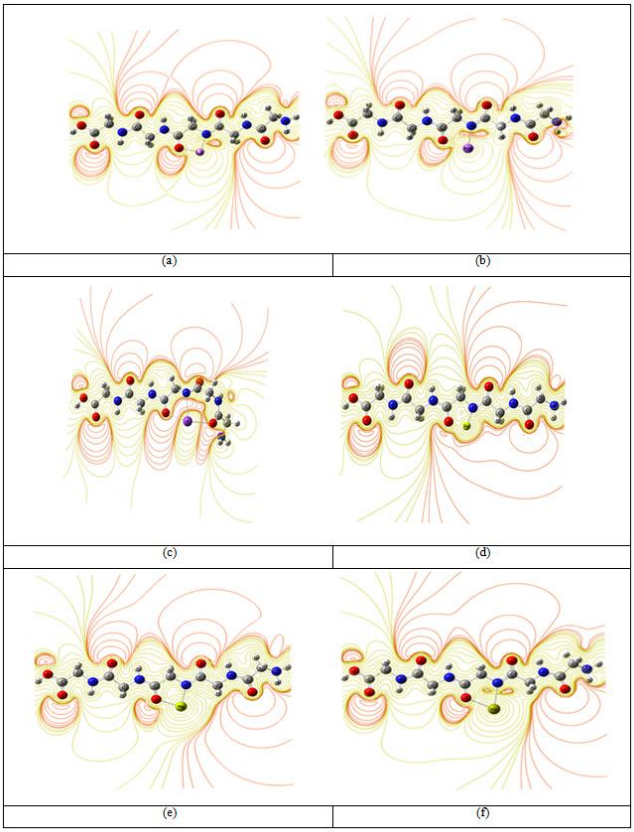

Figure 9. B3LYP B3LYP/6-31G (d,p) ESP as contour of a: Gly-Li, b: Gly-Na, c: Gly-K, d: Gly-Be, e: Gly-Mg and f: Gly-Ca through middle NH group.

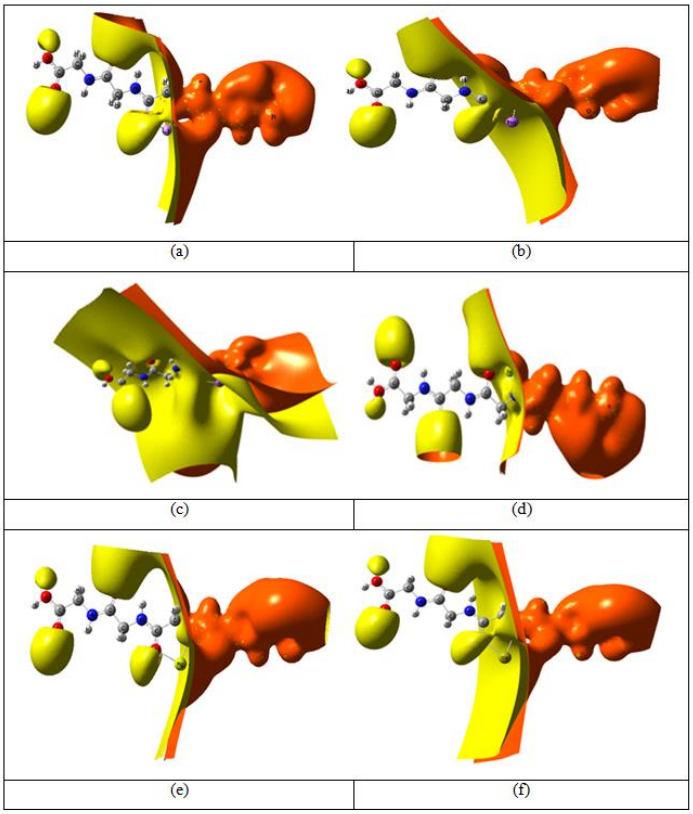

Figure 10. B3LYP B3LYP/6-31G (d,p) ESP as total surface area of a: Gly-Li, b: Gly-Na, c: Gly-K, d: Gly-Be, e: Gly-Mg and f: Gly-Ca through middle NH group.

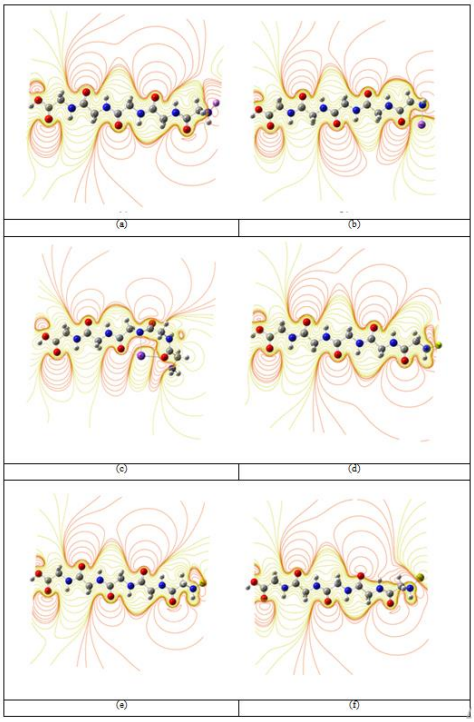

Figure 11. B3LYP/6-31G (d,p) ESP as contour of a: Gly-Li, b: Gly-Na, c: Gly-K, d: Gly-Be, e: Gly-Mg and f: Gly-Ca through terminal amide group.

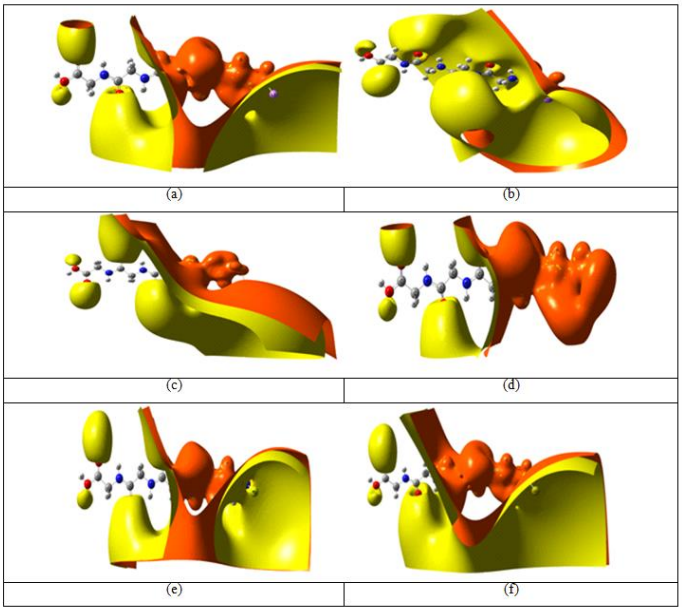

Figure 12. B3LYP/6-31G (d,p) ESP as a total surface of a:Gly-Li, b:Gly-Na, c:Gly-K, d:Gly-Be, e:Gly-Mg and f:Gly-Ca through terminal amide group.

Table 4. B3LYP/6-31G (d,p) calculated bond length and bond angle for the studied structures: a: Gly, b: Gly-Li, c: Gly-Na, d: Gly-K, e: Gly-Be, f: Gly-Mg and g: Gly-Ca through hydroxyl group (chain O), middle NH group (middle N) and finally through terminal amide group (Chain-NH) where X= H, Li, Na, K, Be, Mg and Ca respectively.

Structure	Bond length			Bond angle			
	Terminal OH (O37-X38)	Middle NH (N20-X38)	Terminal amide group (N36-X38)	Terminal OH (X38 O37 C32)	Middle NH (X38N20C3)	(X38 N20 C19)	Terminal amide group H16-N5-X1
Gly	0.9725	1.0149	1.0191	107.013	123.114	114.764	107.697
Gly-Li	1.8671	1.8660	1.7496	82.862	140.498	106.212	117.505
Gly-Na	2.1962	2.2037	2.1971	87.288	129.952	110.679	108.770
Gly-K	2.5378	2.6840	2.5617	91.253	109.316	113.377	120.124
Gly-Be	1.4470	1.1689	1.4991	135.910	134.896	110.628	119.740
Gly-Mg	2.0674	2.0490	1.9259	87.952	134.240	112.919	117.594
Gly-Ca	2.3686	2.4011	2.2550	91.166	132.193	115.978	116.256

4. CONCLUSIONS

DFT level of theory proves to be effective in studying and following up the structural and electronic properties of Gly and is in a good agreement with previous work applied for different other materials [32-36].

Based on the results obtained above for TDM, HOMO/LUMO band gap energy and ESP of the three different mechanisms of interaction, we can conclude that since the decrease in HOMO/LUMO band gap energy values as a result of interaction with alkaline earth metals is much higher than that with alkali metals when the interaction proceeds through both the hydroxyl group and middle NH group, therefore Ca is the highest probable choice for interaction with Gly which means that Ca is much more active in comparison with the rest of the studied metals as HOMO/LUMO band gap energy decreased from 5.2829 eV to 1.7693 and 1.7641 eV.

On the other hand, as HOMO/LUMO band gap energy decreases with increasing atomic number of the doping metals, we can choose K as the best dopant metal if the interaction was done via the terminal amide group and this choice is because the HOMO/LUMO band gap energy significantly decreased until it reached 1.9255 eV.

5. REFERENCES

[1] Cooper T.G., Day G.M., Jones W., Motherwell W.D.S., Crystal structure prediction of the series of α-amino acids, *Acta Cryst*., A62, s229, **2006**.

[2] Grosser N., Oberle S., Berndt G., Erdmann K., Hemmerle A., Schröder H., Antioxidant action of l-alanine: heme oxygenase-1 and ferritin as possible mediators, *Biochem. Biophys. Res. Commun*, 314, 351-355, **2004**.

[3] Kumar K.S., Raghavalu T., Mathivanan V., Kovendhan M., Sivakumar B., Kumar G.R., Raj S.G., Mohan R., Structural, optical, spectral and thermal studies of nonlinear optical pure and deuterated l-alanine single crystals, *J. Cryst. Growth*, 310, 1182-1186, **2008**.

[4] Day G.M., Cooper T.G., Crystal packing predictions of the alpha-amino acids: methods assessment and structural observations, *Cryst. Eng. Comm*., 12, 2443-2453, **2010**.

[5] Reshak A.H., Lakshminarayana G., Kamarudin H., Kityk I.V., Auluck S., Berdowski J., Tylczynski Z., Amino acid 2-aminopropanoic CH 3CH(NH 2)COOH crystals: Materials for photo- and acoustoinduced optoelectronic applications, *J. Mater. Sci-Mater. El.*, 23, 1922-1931, **2012**.
[6] Ignatius I.C., Dheivamalar S., Kirubavathi K., Selvaraju K., Experimental and DFT computational studies of L-alanine cadmium chloride crystals, *Int. J. Comp. Mat. Sci. Eng.*, 5, 1, 1630001, **2016**.
[7] Plimmer R.H.A., Hopkins F.G., eds. *The chemical composition of the proteins*. Monographs on biochemistry. Part I. Analysis (2nd ed.). London: Longmans, Green and Co. 82. *Retrieved January 18*, **2010**.
[8] Sato K., Why does a steep caudal-rostral gradient exist in glycine content in the brain?, *Med. Hypotheses*, 120, 1-3, **2018**.
[9] Betz, H., Glycine receptors: heterogeneous and widespread in the mammalian brain, *Trends Neurosci.*, 14, 10, 458-461, **1991**.
[10] Betz H., Structure and function of inhibitory glycine receptors, *Q Rev. Biophys.*, 25, 4, 381-394, **1992**.
[11] Tanda B.C., Eksteen J.J., Oraby E.A., An investigation into the leaching behaviour of copper oxide minerals in aqueous alkaline glycine solutions, *Hydrometallurgy*, 167, 153-162, **2017**.
[12] Shin D., Ahn J., Lee J., Kinetic study of copper leaching from chalcopyrite concentrate in alkaline glycine solution, *Hydrometallurgy*, In Press, **2018**.
[13] Eksteen J., Oraby E., Process for selective recovery of chalcophile group elements, Australian Provisional Patent Application, #2015900865, **2015**.
[14] Ibrahim M., Koglin E., Vibrational Spectroscopic Study of Acetate Group, *Acta Chim. Slov.*, 51, 453-460, **2004**.
[15] Ibrahim M., Molecular Modeling and FTIR Study for K, Na, Ca and Mg Coordination with Organic Acid, *J. Comput. Theor. Nanosci.*, 6, 3, 682-685, **2009**.
[16] Ibrahim M., Nada A., Kamal, D-E., Density functional theory and FTIR spectroscopic study of carboxyl group, *Indian J. Pure Appl. Phy.*, 43, 911-917, **2005**.
[17] Al-Fifi Z., Eid M., Ibrahim M., On the Spectroscopic Analyses of Protein, *J. Comput. Theor. Nanosci*, 10, 2375-2379, **2013**.
[18] Elhaes H., Elkashef N.M., Abdel-Gawad F.Kh., Shaban A.M., Ibrahim M., Effect of Divalent Metals on the Molecular Structure of Protein: Modeling and Spectroscopic Approaches, *J. Comput. Theor. Nanosci.* 11, 4, 1081-1085, **2014**.
[19] Mandal S., Das G., Askari H., Amino acid-type interactions of L-3,4-dihydroxyphenylalanine with transition metal ions: An experimental and theoretical investigation, *J. Mole. Struct.*, 1100, 162-173, **2015**.
[20] Remelli M., Nurchi V.M., Lachowicz J.I., Medici S., Zoroddu M.A., Peana M., Competition between Cd(II) and other divalent transition metal ions during complex formation with amino acids, peptides, and chelating agents, *Coord, Chem. Rev.*, 327–328, 55-69, **2016**.
[21] Xu X-Y., Yan B., Selective detection and controlled release of Aspirin over fluorescent amino-functionalized metal–organic framework in aqueous solution, *Sensor Actuat. B-Chem.*, 230, 463-469, **2016**.
[22] Ammar N.S., Elhaes H., Ibrahim H.S., El-hotaby W., Ibrahim M.A., A Novel Structure for Removal of Pollutants from Wastewater, *Spectrochim. Acta A.*, 121C, 216-223, **2014**.
[23] Elhaes H., Osman O., Ibrahim M., Interaction of Nano Structure Material with Heme Molecule: Modelling Approach, *J. Comput. Theor. Nanosci.*, 9, 901–905, **2012**.
[24] Abdel-Gawad F.K., Osman O., Bassem S.M., Nassar H.F., Temraz T.A., Elhaes H., Ibrahim M., Spectroscopic Analyses and Genotoxcity of Dioxins in the Aquatic Environment of Alexandria, *Mar. Pollut. Bull.*, 127, 618-625, **2018**.
[25] Galal A.M.F., Shalaby E.M., Abouelsayed A., Ibrahim M.A., Al-Ashkar E., Hanna A.G., Structure and absolute configuration of some 5-Chloro-2-methoxy-N-phenylbenzamide derivatives, *Spectrochim. Acta A.*, 188, 213-221, **2018**.
[26] Gaussian 09, Revision C.01, Frisch M., Trucks G., Schlegel H., Scuseria G., Robb M., Cheeseman J., Scalmani G., Barone V., Mennucci B., Petersson G., Nakatsuji H., Caricato M., Li X., Hratchian H., Izmaylov A., Bloino J., Zheng G., Sonnenberg J., Hada M., Ehara M., Toyota K., Fukuda R., Hasegawa J., Ishida M., Nakajim T., Honda Y., Kitao O., Nakai H., Vreven Y., Montgomery J., Peralta J.Jr., Ogliaro F., Bearpark M., Heyd J., Brothers E., Kudin K., Staroverov V., Keith T., Kobayashi R., Normand J., Raghavachari K., Rendell A., Burant J., Iyengar S., Tomasi J., Cossi M., Rega N., Millam J., Klene M., Knox J., Cross J., Bakken V., Adamo C., Jaramillo J., Gomperts R., Stratmann R., Yazyev O., Austin A., Cammi R., Pomelli C., Ochterski J., Martin R., Morokuma K., Zakrzewski V., Voth G., Salvador P., Dannenberg J., Dapprich S., Daniels A., Farkas O., Foresman J., Ortiz J., Cioslowski J., Fox D., Gaussian, Inc., Wallingford CT, **2010.**
[27] Becke A.D., Density-functional thermochemistry. III. The role of exact exchange, *Chem. Phys*., 98, 5648-5652, **1993**.
[28] Lee C., Yang W., Parr R.G., Development of the Colle-Salvetti correlation-energy formula into a functional of the electron density, *Phys. Rev. B*, **1998**, 37(2), 785.
[29] Miehlich B., Savin A., Stoll H., Preuss H., Results obtained with the correlation energy density functionals of becke and Lee, Yang and Parr, *Chem. Phys. Lett.*, 157, 3, 200-206, **1989**.
[30] Ibrahim M., El-Haes H., Computational spectroscopic study of copper, cadmium, lead and zinc interactions in the environment, *Int. J. Environ. Pollut.*, 23, 4, 417-424, **2005**.
[31] Ibrahim M., Mahmoud A-A., Computational Notes on the Reactivity of Some Functional Groups, *J. Comput. Theor. Nanosci.*, 6, 1523-1526, **2009**.
[32] Dedkov Y., Voloshina E., Spectroscopic and DFT studies of graphene intercalation systems on metals, *J. Electron. Spectrosc.*, 219, 77-85, **2017**.
[33] Üngördü A., Tezer N., DFT study on metal-mediated uracil base pair complexes, *J. Saudi Chem. Soc.*, 21(7), 837-844, **2017**.
[34] Khoutoul M., Lamsayah M., Al-blewi F. F., Rezkib N., Aouad M. R., Mouslim M., Touzani R., Liquid–liquid extraction of metal ions, DFT and TD-DFT analysis of some 1,2,4-triazole Schiff Bases with high selectivity for Pb(II) and Fe(II), *J. Mol. Struct.*, 1113, 99-107, **2016**.
[35] Fischer M., DFT-based evaluation of porous metal formates for the storage and separation of small molecules, *Micropor. Mesopor. Mat.*, 219, 249-257, **2016**.
[36] Wang W., Fan L., Wang G., Li Y., CO_2 and SO_2 sorption on the alkali metals doped CaO(100)surface: A DFT-D study, *Appl. Surf. Sci.*, 425, 972-977, **2017**.